World Journal of Advanced Engineering Technology and Sciences
eISSN: 2582-8266
Cross Ref DOI: 10.30574/wjaets
Journal homepage: https://wjaets.com/

(REVIEW ARTICLE)

Check for updates

Comparative performance analysis of PID and sliding mode controllers in speed control of permanent magnet synchronous motor

James Ukaraobong Cletus, Anyanime Tim Umoette, Ekom Enefiok Okpo and Imo E. Nkan *

Department of Electrical and Electronic Engineering, Faculty of Engineering, Akwaibom state University, Nigeria.

World Journal of Advanced Engineering Technology and Sciences, 2025, 15(03), 2655-2670

Publication history: Received on 17 May 2025; revised on 23 June 2025; accepted on 26 June 2025

Article DOI: https://doi.org/10.30574/wjaets.2025.15.3.1177

Abstract

This paper presents the design and analysis of nonlinear controllers aimed at enhancing the performance of a Permanent Magnet Synchronous Motor (PMSM). A 3-phase, 900kW, 50Hz, 6-pole, 380 V, 756RPM PMSM with 48 rotor slots was modelled using MATLAB/Simulink and ANSYS. The study evaluates the motor transient and steady-state behavior in terms of torque, speed and current under different load conditions, with and without controller integration. Simulation result demonstrates that introducing controllers, particularly the Sliding Mode Controller (SMC), effectively reduces electromagnetic torque and output power ripple while achieving a faster response to steady state compared to the Proportional Integral Derivative (PID) controller. The SMC further enhances speed performance by increasing the load angle during rated operation, thus shifting the pull-out torque to power angle greater than 900. Maximum speed, torque, and current were achieved under 4Nm and 9Nm load conditions. The significance of this performance enhancement is underscored in applications such as robotics and conveyor systems, where variable speed operation is essential. Since PMSM speed is directly related to supply frequency and inversely to the number of poles, speed regulation is constrained by the number of pole-changing methods. Frequency variation remains the most effective approach for wide range speed control. The result obtained indicates that nonlinear control strategies offer superior performance over conventional methods, contributing to a more robust and responsive PMSM speed control system for industrial applications.

Keywords: Permanent Magnet Synchronous Machine (PMSM); Nonlinear Controllers; MATLAB/Simulink; Sliding Mode Controller; Proportional Integral Derivative Controllers (PID); Transient and Steady State Behavior

1. Introduction

Permanent Magnet Synchronous Motors (PMSMs) have emerged as the leading choice for high performance electric drive applications due to their superior power density, high efficiency and low toque ripple especially under high-speed operating conditions [1]. Compared to traditional AC motors, PMSMs exhibit significant advantages such as compact size, absence of rotor copper losses, and high reliability stemming from their brushless construction and use of permanent magnets on the rotor. These attributes makes them particularly suitable for automotive applications, industrial automation, and precision control systems [1, 2], Electric drives are essential for converting electric energy into mechanical energy in a controlled manner, involving the integration of power electronic converters, electrical machines, sensors, control algorithms, and communication links [3]. With the rise in industrial demand for energy-efficient and compact motor solutions, PMSMs have gained widespread adoption, particularly in applications requiring precise torque and speed control [4, 5]. To achieve a high-performance operation of PMSM drives, several control strategies have been developed [6]. Scalar control techniques such as the V/f method offer simplicity but lack dynamic response and precision required in advanced applications [1, 2, 3]. In contrast, vector control methods, including Field Oriented Control (FOC) and Direct Torque Control (DTC), enabled decoupled control of flux and torque, thereby

* Corresponding author: Imo E. Nkan

enhancing transient performance and stability [4, 7, 8]. Among these, DTC has gained attention for its fast torque response and reduced parameters sensitivity. In principle, any voltage vector within the selection region can be used to control stator flux and torque, but the voltage vector's angle has a distinct effect on motor's dynamic performance [9, 10]. The use of voltage vector as a control variable enhances drive performance. However, the direct control of torque in PMSMs introduces complexities due to their inherent coupling between torque and flux components. This coupling necessitates advanced control algorithms for decoupling, which simplifies implementation and improves performance [11, 12]. Additionally, due to the cost and reliability constraints associated with mechanical sensors, sensor-less control schemes have gained prominence. Sensor-less DTC of PMSMs, while promising, demands robust estimation techniques to ensure a stable operation over a wide range of speeds and load conditions [13, 14]. This work investigates the performance of vector control PMSMs using both Proportional-Integral-Derivative (PID) and Sliding Mode Controllers (SMC). The goal is to enhance the speed regulation and dynamic performance of PMSM drives in various operating conditions, particularly under sensor-less scenarios, making them more suitable for industrial applications that demand precision, efficiency, and robustness [15, 16].

1.1. Permanent Magnet Synchronous Motor (PMSM)

Permanent Magnet Synchronous Motors (PMSMs) are brushless AC motors characterized by high efficiency, high power density, and superior reliability [17]. The use of permanent magnet in the rotor eliminates the needs for rotor windings and associated losses, enabling a higher torque to weight ratios and compact designs compared to AC Induction Motors (AICMs). PMSMs operates with rotor speed synchronized to the stator's rotating magnetic field, maintaining constant speed regardless of load variations [18, 19]. It is ideal for precision and efficiency-critical applications such as electric and hybrid vehicles. Ac motor s is generally classified into asynchronous (induction) and synchronous types. Induction motors, or separately excited machines, rely solely on stator fed AC supply, with rotor excitation achieved through electromagnetic induction in contrast synchronous motors require AC excitation for the stator and typically a DC or permanent magnet excitation for the rotor [20]. The speed of a synchronous motor is fixed by the supply frequency and number of poles, unaffected by the load changes. Three phase PMSM are adopted in industrial drives due to their robustness, cost effectiveness and low maintenance requirements. While sometimes confused with synchronous machines, PMSMs are true synchronous machines, differing fundamentally in their operation principles and performance characteristics [4].

Permanent magnet synchronous machine shares the fundamental operation principles and performance characteristics of conventional synchronous machines, with excitation provided by permanent magnets rather than a wound field winding. A typical PMSM comprises a laminated core whose teeth house double layer, or lap wound armature coils connected in series or parallel to realize star/delta, or two-phase configurations and a salient pole rotor carrying surface or interior mounted permanent magnets [21]. The stator yoke completes the magnetic circuit, and its lamination thickness is chosen to balance eddy current losses (frequency dependent) against manufacturing cost. End turn insulation of coils and phase groups must satisfy the dielectric requirements dictated by machine voltage ratings. The air-gap ln in a PMSM not only determine the no-load flux density established by the permanent magnets but also affects the windage losses.

A permanent synchronous motor (PMSM) comprises two main components: a rotor which rotate and a stator which remain stationary. Typically, the rotor is enclosed within the stator [22]. The fundamental operating principle of a PMSM relies on the interaction between the stator's rotating magnetic field and the rotors constant magnetic field. When a three-phase alternating current is supplied to the stator windings, it generates a magnetic field that rotates at a speed proportional to the supply frequency [23]. The rotor, embedded with permanent magnet, produces astatic magnet field. The interaction between the stator's rotating field and the rotors static field generates torque, as described by Ampere's law, thereby causing thereby causing the rotor to turn. If the rotor is initially in the direction of the stator's magnetic field, opposite magnetic attract, resulting in synchronization between the rotor and stator's rotating fields rotating field. However, due to the nature of its magnetic coupling, a PMSM is inherently incapable of self-starting when directly connected to a three-phase supply [24, 25]. The operation of a synchronous motor, including the PMSM, hinges on this same interaction between the stator's rotating magnetic field and the rotor's magnetic field. The rotating magnetic field in the stator I similar to that produced in a three-phase induction motor. As the stator's AC field interacts with the constant magnetic field of the rotor, torque is produced according to Ampere's law. The permanent magnets on the rotor maintain a constant field. Consequently, without an external starting mechanism, PMSMs cannot self-start when powered by a standard 50Hz three-phase grid [26, 27, 28].

Permanent magnet synchronous moor (PMSM) drives are increasingly utilized in industrial applications where precisions and high accuracy are critical. Due to their superior dynamic performance [29]. PMSM drives are emerging as the leading solution for the next generation electric motor systems. Effective control is essential to ensure optimal

operation, particularly because PMSMs are inherently variable speed machines. The control strategy typically depends on the controller and the algorithm implemented to regulate speed, torque, and rotor position with high accuracy [30, 31]. The key control techniques include: Flux weakening control, Constant torque angle control, unity power factor control, Maximum torque per ampere (MTPA)control, Constant power loss control, Maximum efficiency control. These methods aimed to enhance performance by improving motor dynamic and steady state behaviour. Among the various approaches, vector control and direct torque control are the most prominent and widely adopted strategies for high performance PMSM operation [32, 33, 34].

2. PMSM Model

The PMSM's equivalent circuit is depicted in Figure 1. Equations 1 through 12 illustrate the motor's voltage, current, and flux linkage in the model equations [35].

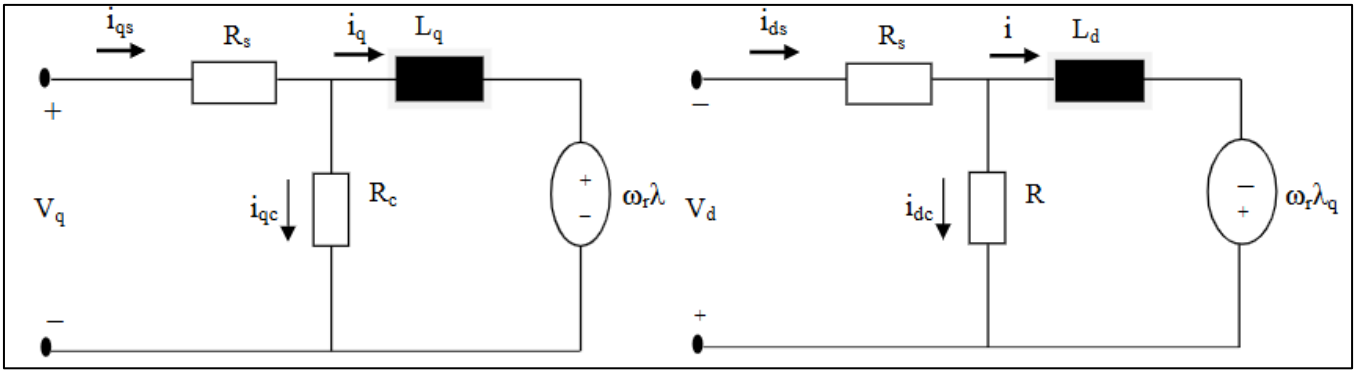

Figure 1 Equivalent circuit of PMSM

The axis voltage equations can be written as

$$v_q = R_s i_q + \frac{R_s + R_c}{R_c}\rho(\gamma_q) + \frac{R_s + R_c}{R_c}\omega_r \gamma_d \quad \text{..... (1)}$$

$$v_d = R_s i_d + \frac{R_s + R_c}{R_c}\rho(\gamma_q) + \frac{R_s + R_c}{R_c}\omega_r \gamma_q \quad \text{..... (2)}$$

Where the axis flux linkages in the rotor reference frame are given by

$$\lambda_q = L_q i_q \quad \text{..... (3)}$$

$$\lambda_d = L_d i_d \gamma_m \quad \text{..... (4)}$$

Substituting equations (3) and (4) into equations (1) and (2), we have

$$v_q = R_s i_q + \frac{(R_s + R_c)}{R_c}\rho(L_q i_q) + \frac{(R_s + R_c)}{R_c}\omega_r (L_d i_d + \gamma_m) \quad \text{..... (5)}$$

$$\frac{di_q}{dt} = \frac{-R_s R_c}{R_q(R_s + R_c)} i_q - \frac{\omega_r R_c}{L_d}(i_q) + \frac{V_q R_c}{L_q(R_s + R_c)} - \frac{\omega_r \gamma_m}{L_q} \quad \text{..... (6)}$$

$$v_d = R_s i_q + \frac{(R_s + R_c)}{R_c}\rho(L_q i_q + \gamma_m) - \frac{(R_s + R_c)}{R_c}\omega_r (L_q i_q) \quad \text{..... (7)}$$

$$\frac{di_q}{dt} = \frac{\omega_r L_q}{L_d}(i_q) - \frac{R_s R_c}{L_q(R_s + R_c)} i_q + \frac{V_d R_c}{L_d(R_s + R_c)} \quad \text{..... (8)}$$

Where;

ρ = Operator $\frac{d}{d_t}$

$\rho(\gamma_m) = 0$

V_q *and* V_d: $q - axis$ *and* $d - axis$ *voltages*

$i_q \; and \; i_d$: $q - axis \; and \; d - axis \; current$
L_q and L_q: q − axis and d − axis inductances
$\gamma_q \; and \; \gamma_d$: q − axis and d − axis flux linkages

R_s: Stator resistance

R_c: Core resistance

ω_r: Electrical speed of the rotor

γ_m: Rotor flux linkage

The general mechanical equation for the motor is

$$T_e = T_l + T_d + B_{\omega_{rm}} + \text{Jρ}\omega_{rm} \qquad \text{…….. (9)}$$

Electromagnetic torque of the motor in terms of d-axis and q-axis flux linkages, rotor flux linkage, and d- axis and q-axis inductances is given as:

$$T_e = \frac{3}{2}(\frac{P}{2})(\gamma_d i_q - \gamma_q i_d) \qquad \text{…….. (10)}$$

Substituting Equations (3) and (4) into Equation 10 gives

$$T_e = \frac{3}{2}(\frac{P}{2})(\gamma_m i_q + (L_d - L_q)\, i_q i_d \qquad \text{…….. (11)}$$

Solving for the rotor mechanical speed from Equation (9), assuming the dry friction is equals zero gives

$$\frac{d\omega_{rm}}{dt} = \frac{-B}{J}\, \omega_{rm} + \frac{1}{j}(T_e - T_i) \qquad \text{…….. (12)}$$

also,

$$\frac{d\theta_r}{dt} = \omega_r \qquad \text{…….. (13)}$$

The Electromechanical power is given as

$$P_{em} = \omega_{rm} T_e = \frac{3}{2}\omega_r(\gamma_d i_q - \gamma_q i_d) \qquad \text{…….. (14)}$$

$$\omega_r = \frac{P}{2}\omega_{rm} \text{……..(15)}$$

The mechanical speed N (that is synchronous speed) in terms of revolutions per minute (rpm) can be stated as

$$N = \frac{30}{\pi} \times \omega_{rm} \qquad \text{…….. (16)}$$

where:

P: Number of poles

- ω_{rm}: Mechanical velocity of the motor
- B: Viscous frictions coefficient
- J: Inertia of the shaft and the load system
- T_d: Dry friction
- T_L: Load torque
- T_e: Electromagnetic torque
- θ_r: Electrical Rotor angular position

- θ_m: Mechanical Rotor angular position
- N: Synchronous speed.

Combining Equations (6), (8), (12), and (13) in state variable form gives

$$\frac{d}{dt}\begin{bmatrix} i_q \\ i_d \\ \omega_{rm} \\ \theta_r \end{bmatrix} = \begin{bmatrix} \frac{-R_s R_c}{L_q(R_s+R_c)} & \frac{-\omega_r L_d}{L_q} & 0 & 0 \\ \frac{\omega_r L_d}{L_q} & \frac{-R_s R_c}{L_q(R_s+R_c)} & 0 & 0 \\ 0 & 0 & \frac{-B}{J} & 0 \\ 0 & 0 & 0 & 0 \end{bmatrix} \begin{bmatrix} i_q \\ i_d \\ \omega_{rm} \\ \theta_r \end{bmatrix} + \begin{bmatrix} \frac{1}{L_q}\left(\frac{V_q R_C}{R_s - R_c} - \omega_r \lambda_m\right) \\ \frac{V_d R_c}{L_q(R_s+R_c)} \\ \frac{1}{j}(T_e - T_i) \\ \omega_r \end{bmatrix} \quad .. (17)$$

PMSM can be analyzed in both steady and transient state operations using the dynamic dq equations. This is accomplished by applying Park's transformation method to convert the three-phase voltages and currents to dq variables [36].

The reference frame voltages of PMSM under the condition of balance state can be estimated as:

$$V_a - \sqrt{2}V cos\omega_b t \quad \text{..... (18)}$$

$$V_b - \sqrt{2}V cos(\omega_b t - \tfrac{2\pi}{3}) \quad \text{..... (19)}$$

$$V_b - \sqrt{2}V cos(\omega_b t + \tfrac{2\pi}{3}) \quad \text{..... (20)}$$

2.1.1. Were

$\omega_b = 2\pi f$ is the rated source frequency in rad/s

V_a, V_b, and V_c: Stator phase a, b, c voltages

V: Line voltage

The three-phase voltages of the stator circuit are related to q- axis and d-axis reference frame as follows

$$\begin{bmatrix} V_q \\ V_d \end{bmatrix} = \frac{2}{3}\begin{bmatrix} \cos\theta & \cos(\theta - 120°) & \cos(\theta + 120°) \\ \sin\theta & \sin(\theta - 120°) & \sin(\theta + 120°) \end{bmatrix} \begin{bmatrix} V_a \\ V_b \\ V_c \end{bmatrix} \quad \text{..... (21)}$$

$$\begin{bmatrix} V_a \\ V_b \\ V_c \end{bmatrix} = \begin{bmatrix} \cos\theta & \sin\theta \\ \cos(\theta - 120°) & \sin(\theta - 120°) \\ \cos(\theta + 120°) & \sin(\theta + 120°) \end{bmatrix} \begin{bmatrix} V_q \\ V_d \end{bmatrix} \quad \text{..... (22)}$$

Also, the three phase currents can be evaluated in the same way as

$$\begin{bmatrix} I_q \\ I_d \end{bmatrix} = \frac{2}{3}\begin{bmatrix} \cos\theta & \cos(\theta - 120°) & \cos(\theta + 120°) \\ \sin\theta & \sin(\theta - 120°) & \sin(\theta + 120°) \end{bmatrix} \begin{bmatrix} I_a \\ I_b \\ I_c \end{bmatrix} \quad \text{..... (23)}$$

$$\begin{bmatrix} I_a \\ I_b \\ I_c \end{bmatrix} = \begin{bmatrix} \cos\theta & \sin\theta \\ \cos(\theta - 120°) & \sin(\theta - 120°) \\ \cos(\theta + 120°) & \sin(\theta + 120°) \end{bmatrix} \begin{bmatrix} I_q \\ I_d \end{bmatrix} \quad \text{..... (24)}$$

Where I_a, I_b, and I_c are the stator phase a, b, c currents while θ is the phase angle. The block diagram of FOC in PMSM is presented in Fig 2.

3. Sliding mode Controller Design

When a sliding mode controller is used, the system is managed so that the error in its states consistently approaches a sliding outside. The state's rate of change ($\dot{e}$) and tracking error (e) are variables used to define the sliding surface. To

determine the control input (u) to the system, the error trajectory's distance from the sliding surface and its rate of convergence are used. When the sliding surface and the tracking error trajectory intersect, the control input's sign needs to change. This forces the error trajectory to always go in the direction of the sliding surface

An equivalent description of the mechanical equation under full field-oriented control is as follows:

$$T_e = K_T i_{qs} \text{..... (25)}$$

K_T is constant torque

$$K_T = \frac{3PL_m}{4L_r}\varphi_{dr} \quad \text{..... (26)}$$

The mechanical equation of induction motor is given as:

$$T_e = \mathrm{J}_{\dot{\omega}\dot{m}} + \mathrm{B}_{\omega\dot{m}} + T_L \quad \text{..... (27)}$$

From equation (25) and equation (27) we have:

$$bi_{qs} = \omega\dot{m} + a\omega\dot{m} + f \quad \text{..... (28)}$$

$$a = \frac{\mathrm{B}}{\mathrm{J}}, \qquad b = \frac{\mathrm{K}}{\mathrm{T}}, \quad f = \frac{T_L}{\mathrm{J}}$$

From equation (22) the Δa , Δb , Δf are uncertainties

$$\omega_{\dot{m}} = -(\mathrm{a} + \Delta\mathrm{f})\omega - (\mathrm{a} + \Delta\mathrm{f}) + (\mathrm{b} + \Delta\mathrm{b})\mathrm{iqs} \quad \text{..... (29)}$$

Tracking speed errors is defined as:

$$e(t) = \omega_m(t) - \omega_m * (t) \quad \text{..... (30)}$$

Where $\omega m *$ is the reference speed, taking derivative of equation (30)

$$\dot{e}(t) = \omega_{\dot{m}}(t) - \omega_{\dot{m}} * (t) \quad \text{..... (31)}$$

Also

$$\dot{e}(t) = -ae(t) + u(t) + d(t)$$

Where:

$$u(t) = bi_{qs} - a\omega_m * (t) - f(t) - \omega_{\dot{m}} * (t) \quad \text{..... (32)}$$

And the uncertainties become:

$$d(t) = -\Delta a\omega_m(t) - \Delta f(t) + \Delta bi_{qs} \quad \text{..... (33)}$$

Sliding mode surface is in equation (34)

$$s(t) = e(t) - \int_0^t (k - a)e(\tau)d\tau \quad \text{..... (34)}$$

Where k is a constant gain, whether sliding mode occur on the sliding surface,

then $s(t) = \dot{s}(t) = 0$, which amount to equation (35)

$$\dot{e}(t) = (k - a)e(t) \quad \text{..... (35)}$$

In order to obtain the speed trajectory tracking, k must be chosen so that the term $(k - a)$ is strictly negative and hence $k < 0$, therefore the sliding surface is defined as:

$$s(t) = e(t) - \int_0^t (k - a)e(\tau)d\tau = 0 \qquad \ldots\ldots\ldots\ldots\ldots (36)$$

The variable structure controller is design as in equation (37)

$$u(t) = ke(t) - \beta sgn(S) \qquad \ldots\ldots\ldots\ldots\ldots (37)$$

Where β is a switching gain, S is the sliding variable and $sgn(S(t))$ is the sign function defined as:

$$sgn\big(S(t)\big) = \begin{cases} 1 & if\ s(t)>0 \\ -1 & if\ s(t)<0 \end{cases} \qquad \ldots\ldots\ldots\ldots\ldots (38)$$

also, the gain β must be chosen so that $\beta \geq |d(t)|$all the time

When sliding mode occurs on the sliding surface, then $S(t) = S(t) = 0$ and the tracking error converges to zero exponentially. From (32) and (37), the current command $iqs*$ can be obtained as

$$i_{qs}*(\mathrm{t}) = \frac{1}{b}[\mathrm{ke} - \beta\mathrm{sgn(S)} + \mathrm{a}\omega_m * (\mathrm{t}) + \omega_{\dot{m}} * (\mathrm{t}) + f] \qquad \ldots\ldots\ldots\ldots\ldots (39)$$

And the value of the current sent to the motor from the controller is given in equation (39), for the command reference speed [37].

4. Reduction of Chattering

To achieve satisfactory tacking performance with a sliding mode controller, the value of β must be large in a system with higher modelling imperfection, parameter variations, and noise levels. Nevertheless, a higher value of β causes the control variable and system states to chatter more. To lessen chattering, a boundary layer with a defined width is added on both sides of the switching line. As illustrates in flow chat of sliding mode controller in Fig. 2, the width of the boundary layer is on either side of the switching line. The control law in equation (37) is changed to:

$$u(t) = ke(t) - \beta sgn\frac{s}{\emptyset} \qquad \ldots\ldots\ldots\ldots\ldots (40)$$

Where:

$$sat\frac{s}{\emptyset} = \begin{cases} \frac{s}{\emptyset} & if \quad |s| \leq \emptyset \\ sgn(s) & |a| > \emptyset \end{cases} \qquad \ldots\ldots\ldots\ldots\ldots (41)$$

The proposed flowchart for sliding mode controller is shown in Fig. 2.

4.1. Design of PID Controller

The MATLAB tool is utilized to effectively search for the system's ideal PID controller parameters. Better features of this method include less computational work and ease of implementation [38, 39]. The PID controller's block diagram is displayed in Fig 3.

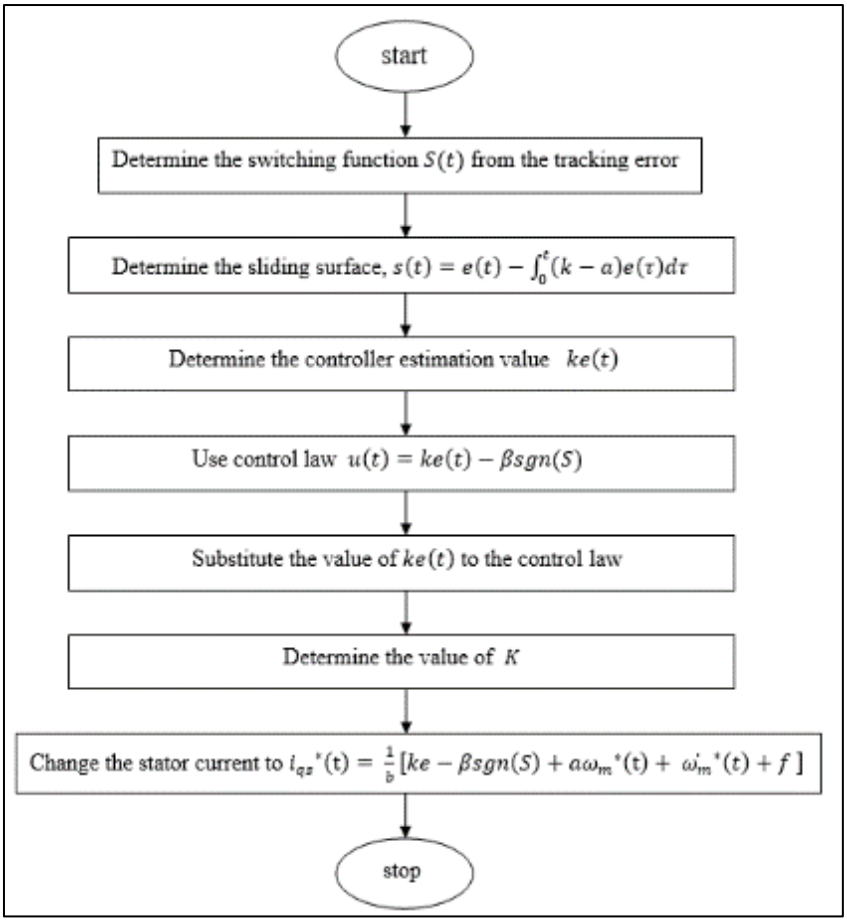

Figure 2 Flow chat of sliding mode controller development

As shown in Fig 3, the PID controller's output, u (t), is the sum of three signals: the signal produced by differentiating and multiplying the error signal by a constant derivative gain, kD; the signal produced by integrative control response; and the signal produced by multiplying the error signal by a constant proportional gain, kp. The final form of the PID algorithm is displayed in equation (42), where $u(t)$ is defined as the controller output.

$$ut = k_p.e(t) + k_i \int e(t)dt + k_d \frac{de(t)}{dt} \quad \text{.....} \quad (42)$$

4.1.1. Were

- k_p: Proportional gain, a tuning parameter
- k_i: Integral gain, a tuning parameter
- k_d: Derivative gain, a tuning parameter
- e: Error
- t: Time or instantaneous time (the present)

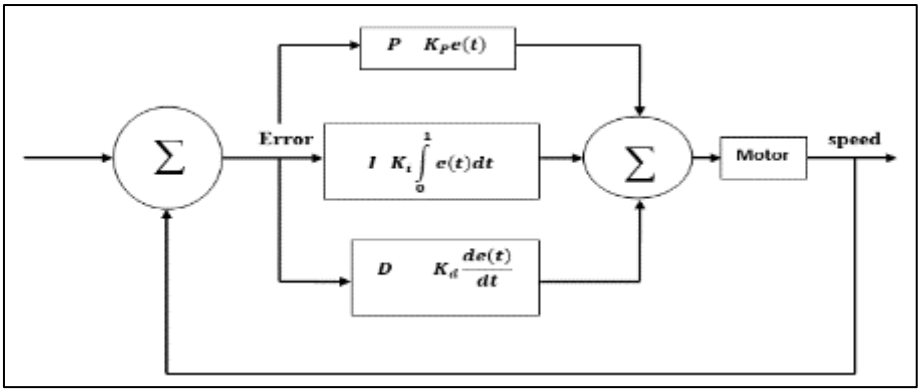

Figure 3 Block diagram of PID controller

- A MATLAB tool is used to design the tuning mechanism, which can change the PID parameters to regulate the motor's speed and determine the transfer function of the intricate SCIM.
- The optimal dynamic performance was achieved by achieving a fixed PID gain of 1.3, 87.1, and 0.004 following a successful trial-and-error method of controller tuning.

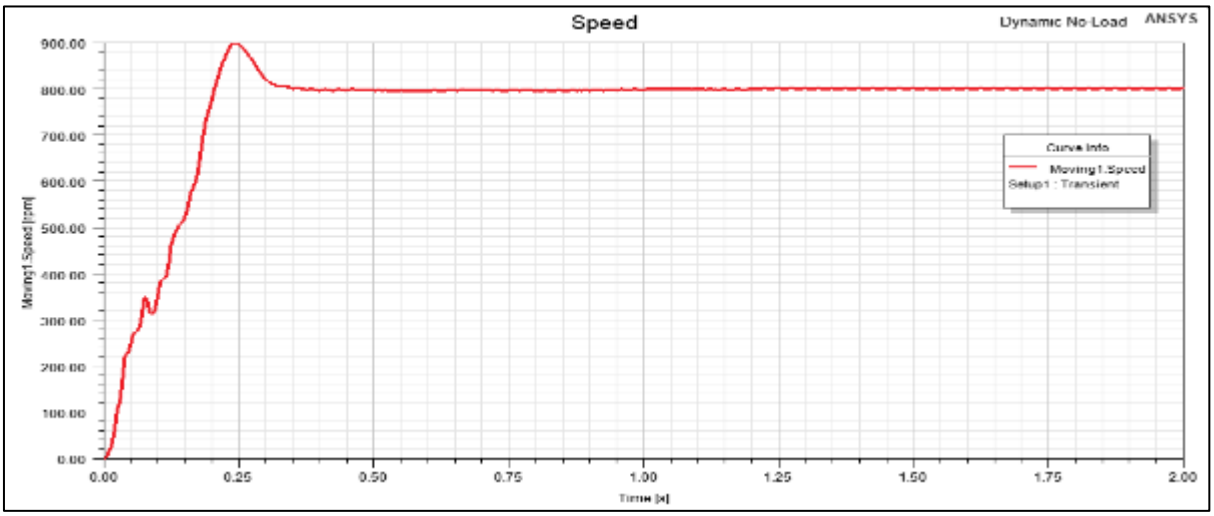

Figure 4 Speed response of PMSM at no-load

5. Simulation results and discussions

The Simulation results and discussions includes the steady state and dynamic state results of PMSM without and with controllers, Dynamic state results with proportional integral differential (PID) and sliding mode controller (SMC). This result has been achieved at different operating conditions such as with and without load (constant and non-linear load) variable reference speed and variable reference load torque. The PMSM data parameters are presented in table 1. MATAB/Simulink was used for both the design and the simulation. The controllers were made specifically to control speed variations with a constant load and intermittent loads with a constant.

Every controller's speed, torque, and current responses were examined, evaluated, and contrasted in terms of overshoot, undershoot, rise time, settling time, and steady state error. In the following sections, the simulation are broken down.

Table 1 Three phase PMSM data parameters

S/N	Parameter	Specification
1	Power rating	900 W
2	Rated speed	1700 RPM
3	Rated Voltage	380
4	Frequency	50
5	Number of poles	6
6	Current rating	16.7 A
7	Number of Rotor slot	48
8	External diameter of stator	210
9	Internal diameter of stator	148
10	Rotor Length	250
11	Internal diameter of Rotor	48
12	Stack Length	0.95
15	Mode of connection	Star

5.1. Dynamic Analysis of PMSM Model Without Controller

This is the Simulink dynamic analysis of the permanent magnet synchronous motor and the Simulink model was build using the parameters of PMSM generated from ANSYS RMxpt software. The behavior of the PMS motor on different conditions were generated from the Simulink model of PMSM. The speed response of the motor at no load is shown in Fig 4. while the response of the speed with 9Nm is shown in Fig 5.

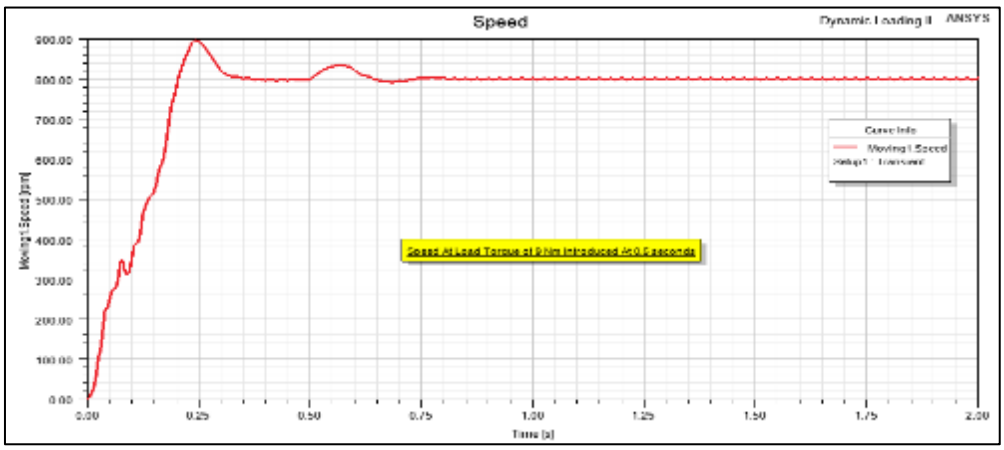

Figure 5 Speed response of PMSM at 9Nm load

5.2. Results under Variable speed and Constant load torque using PID controller

The dynamic performance of the PMSM when a constant load is applied with intermittent speed is presented in this section. In this operating condition 4Nm is driven by varying speed of 0 rad/s and 500rad/s using different controllers. These loads are driven by the motor with 500rpm speeds, and its performance using these controllers (PID, and SMC, are analyzed and compared in term of steady state error, overshoot, undershoot, settling time and rise time. This section presents a dynamic behavior of the motor on variable speed and constant load torque. PMSM with varying speed and Constant load torque using PID controller.

The speed performance of the PMSM drive with PID controller driving 4Nm with a varying speed of 0-500rpm, at 0sec, 0.5 sec and I sec respectively is presented in Fig 6. The corresponding electromagnetic torque and current response are shown in Fig. 7 and 8 respectively.

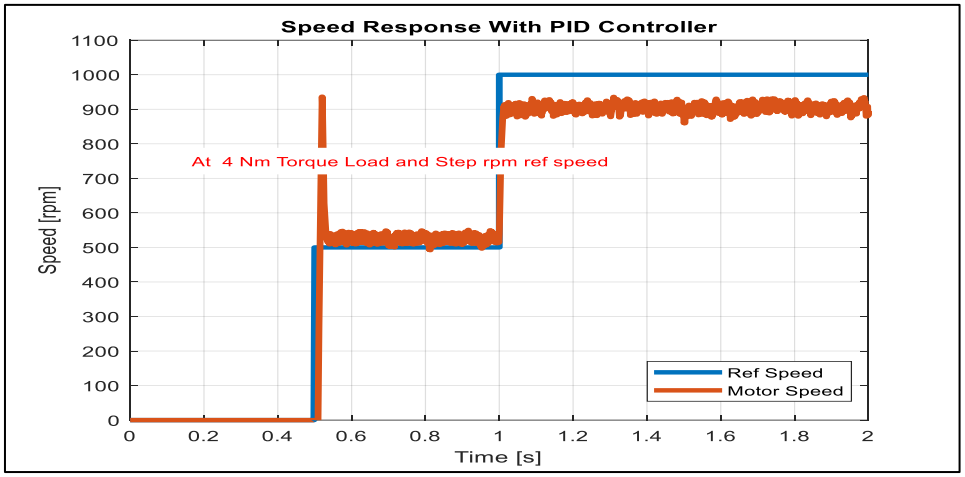

Figure 6 Variable Speed response of PMSM with PID controller

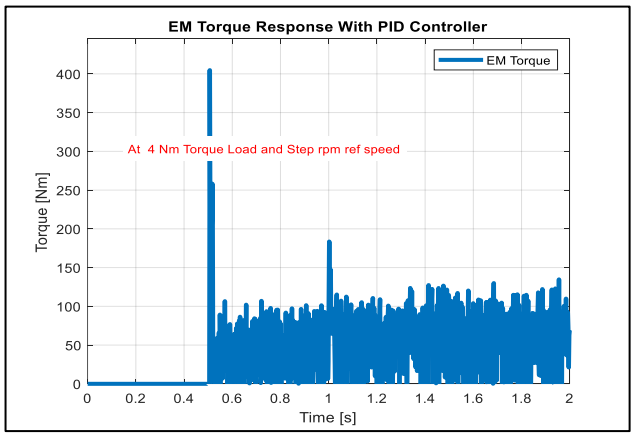

Figure 7 Torque on variable speed respond of of PMSM with PID controller

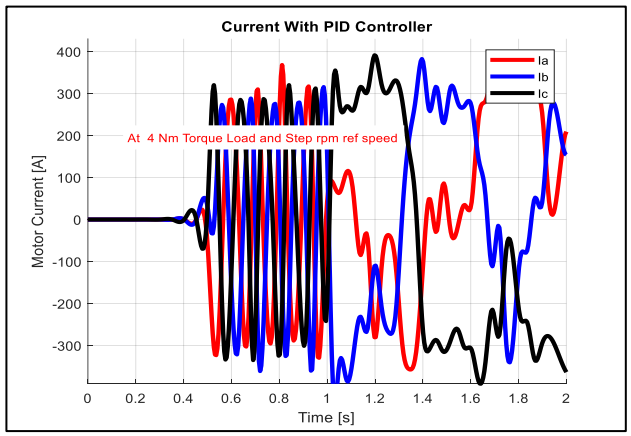

Figure 8 Current on variable speed respond of PMSM with PID controller

5.3. Results under Variable speed and Constant load torque using SM controller

The speed performance of the PMSM drive with SMC driving 4Nm, with a varying speed of 0rad/s, 15rad/s and 30rad/s at 0sec, 0.5 sec and I sec respectively is presented in Fig. 9. The corresponding electromagnetic torque and current response are shown in Fig. 10 and 11 respectively. The summary of the PMSM dynamic performance using SMC with variable speed and constant load torque are presented in Table 2, with variable speed response of PMSM with PID and SM controllers shown in Fig. 12.

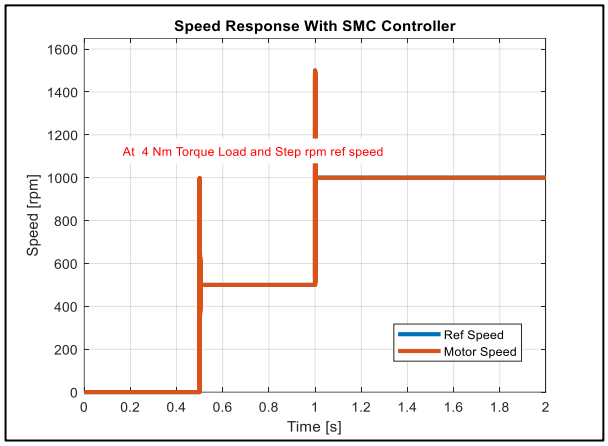

Figure 9 Variable speed respond of PMSM with SM controller

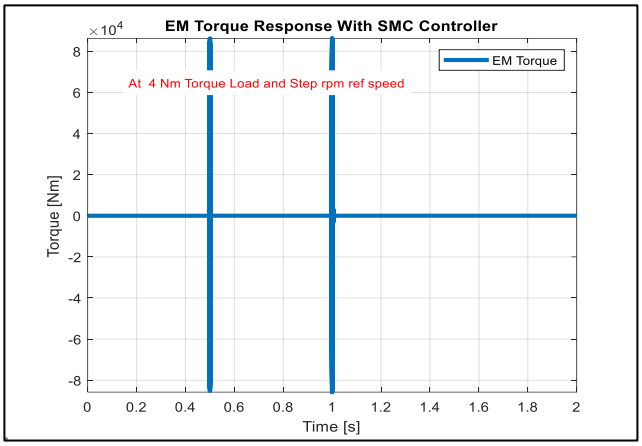

Figure 10 Torque respond on variable speed of PMSM with SM controller

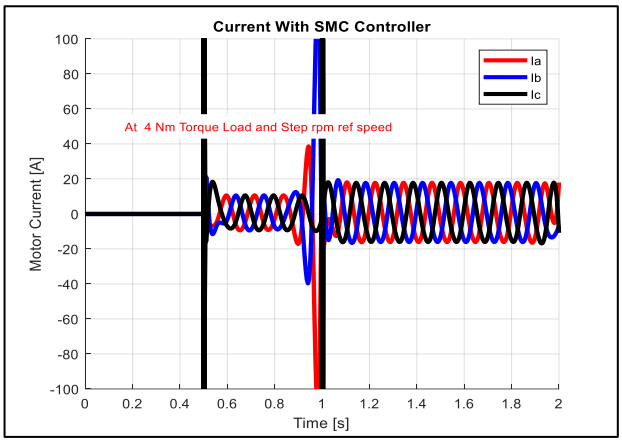

Figure 11 Current respond on variable speed of PID SM controller

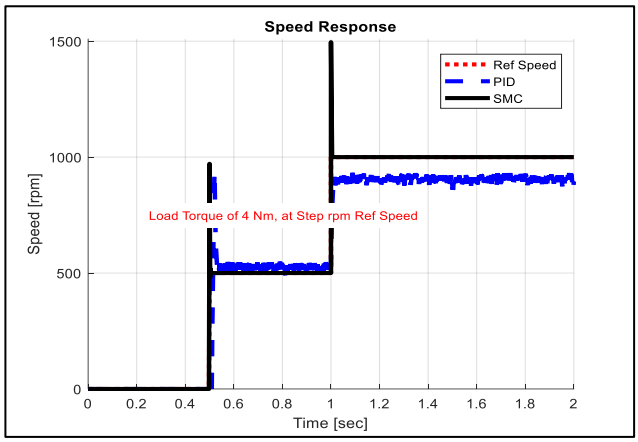

Figure 12 Variable speed respond of PMSM PMSM with SM controller

Table 2 Performance Compares of controllers on variable speed using PID and SM controllers

Controller	Load	Steady State Error (%)	Overshoot (%)	Settling Time (sec)	Rise Time (sec)	Undershoot [%]
SMC	4Nm	2.3528	0.23551	0.0023038	0.0011284	0
PID	4Nm	8.00	12.00	0.22	0.05	0

5.4. Results under step load with constant speed using PID controller

The speed performance of the PMSM drive with PID controller driving 9Nm at 0.5 second with a constant speed of 500rpm is presented in Fig. 13. The corresponding electromagnetic torque and current response are shown in Fig 14, and 15 respectively.

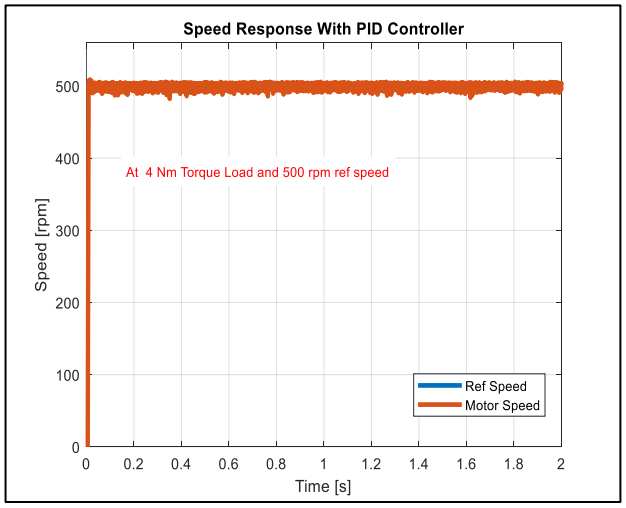

Figure 13 Intermittent speed using PID controller

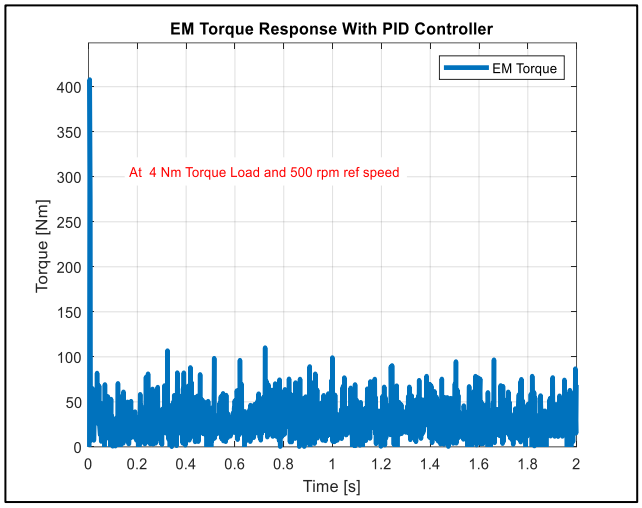

Figure 14 intermittent load torque using PID controller

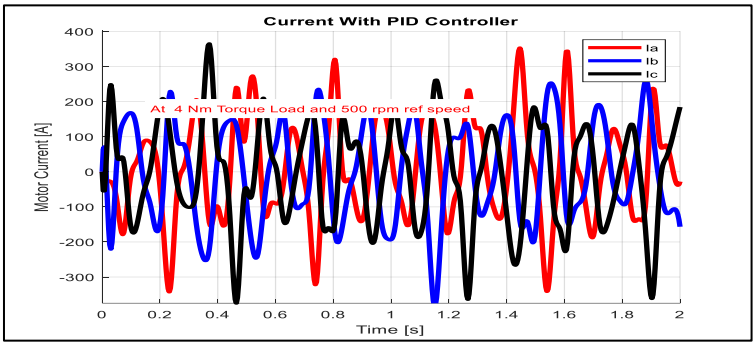

Figure 15 Intermittent current using PID controller

5.5. Results under step load with constant speed using SM controller

The speed performance of the PMSM drive with SMC driving 9Nm at 0.5 second with a constant speed of 500rad/s is presented in Fig 16. The corresponding electromagnetic torque, current response and speed of SM and PID controller are shown in Fig 17, 18, and 19 respectively. The summary of the PMSM dynamic performances using SMC controller with constant speed and variable load torque are presented in table 3.

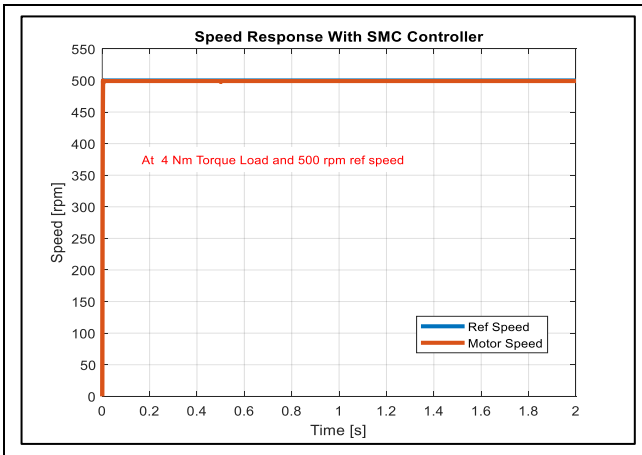

Figure 16 Intermittent current using SM controller

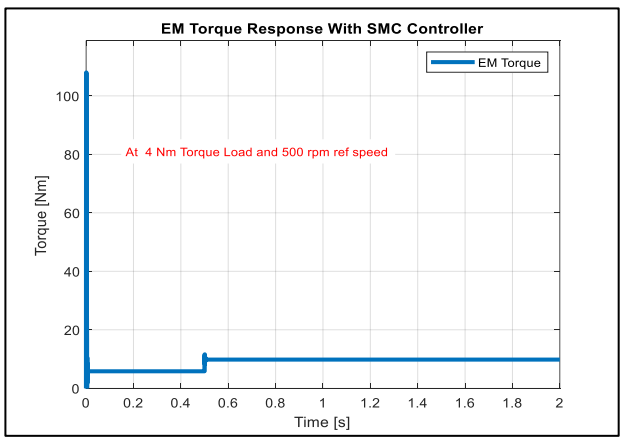

Figure 17 Intermittent load torque using SM controller

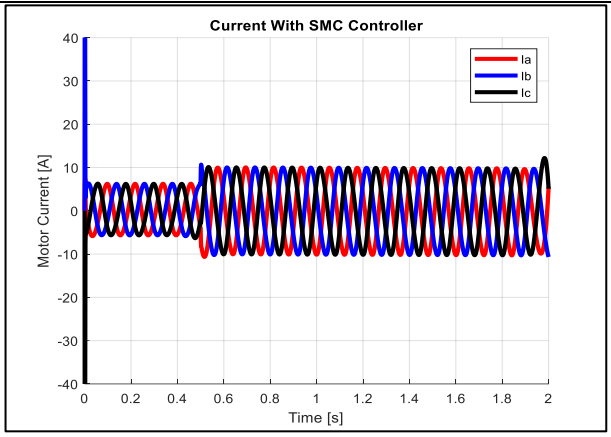

Figure 18 Intermittent current using SM controller

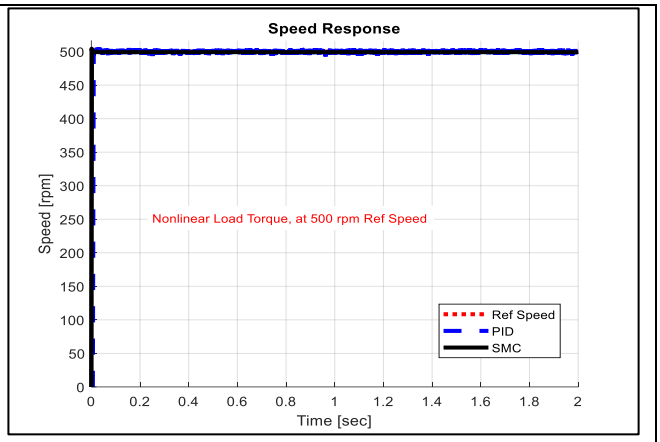

Figure 19 Intermittent speed using PID and SM controller

Table 3 Performance Compares of SMC and PID constant speed and step load torque

Controller	Load	Steady State Error (%)	Overshoot (%)	Settling Time (sec)	Rise Time (sec)	Undershoot [%]
SMC	9Nm	0.84916	0.170	0.0032	0.0021	0
PID	9Nm	4.00	2.0	0.2	0.02	4.00

6. Conclusion

PMSM are mostly used in industrial plants due to their high efficiency, reliability, low maintenance requirements, e.t.c Also, PMSM has delivered same performance as a direct current machine drive in the application that requires speed control since the development of vector control method. In this research, controllers were developed and designed for advance vector speed control technique for PMSM and the dynamic behaviors of the PMSM under the vector control technique these controllers are analyzed. The three phase PMSM was modeled in ANSYS Maxwell. Using the RMexpt platform the steady state behaviors of the motor was studied and the current with the speed, Torque with speed and speed efficiency relationship of the motor were clearly seen. The model designed in RMexpt was transferred to the Maxwell 2D platform for actual dynamic analysis, where the current, electromagnetic torque, and speed wave form were studied for different loading conditions. The data of the motor model in Ansys RMexpt was use to conveniently model the PMSM in MATLAB/Simulink for the actual speed control. The dynamic behavior of the PMSM was analyzed at different load conditions. PID, and SMC were designed in MATLAB/Simulink and used for vector control technique for speed control at different operating conditions.

The operating conditions considered were constant speed on constant load, constant speed on step load, and varying speed on constant load. Non-linear load was also tested on the PMSM the performance of the motor with these controllers were compared in term of steady state error, rise time, settling time, overshoot and undershoot with the operating conditions. When SM controllers was used on a constant speed of 25rad/s and constant load of 4Nm, the steady state, overshoot, settling time, rise time and undershoot were 0.1%, 0.1%, 0.01%sec, 0.01%sec and 0%respectively, speed of 500rad/s and load of 9Nm gives the steady state, overshoot, settling time, rise time and undershoot were, 0.1%, 2%, 0.01sec, 0.01sec and 0% respectively, variable speed of 0rad/s, 10rad/s and 500rad/s and a constant load of 4Nm, the steady state, overshoot, settling time, rise time and undershoot were 0.1%, 4%, 0.05sec, 0.01sec and 32% respectively. From the results, it is established that SM controller has produced the best speed performance on the operating conditions considered, and the error realized with SMC are very negligible that it can be comfortably used in the most sensitive applications.

Compliance with ethical standards

Disclosure of conflict of interest

Authors have declared that no competing interests exist.

References

[1] P. Vas, Artificial Intelligence-based Electrical Machines and Drives, Oxford: Oxford University press, 1999.

[2] P. Krause, Analysis of Electic Machinery, New York: McGraw-Hill, 1986.

[3] L. Zhong, M. F. Rahman, W. Y. Hu and K. W. Lim, "Analysis of Direct Torque Control in Permanent Magnet Synchronous Motor Drives," IEEE Transactions on Power Electronics, vol. 12, pp. 528 -536 , 2017.

[4] J. Luukko, M. Niemelä and J. Pyrhönen, "Estimation of the flux linkage in a direct-torquecontrolled drive," IEEE Trans. Ind. Electron, vol. 50, no. 2, 2003.

[5] A. T. Umoette, O. I. Okoro and I. E. Davidson, "Implementation of indirect field oriented control of a 2.2 kW three-phase induction motor using MATLAB simulink," in In 2021 IEEE AFRICON, 2021.

[6] B. Wu, D. Xu, J. Ji, W. Zhao and Q. Jiang, "Field-oriented control and direct torque control for a five-phase fault-tolerant flux-switching permanent-magnet motor," Chinese Journal of Electrical Engineering, vol. 4, no. 4, pp. 48-56, 2018.

[7] O. Benjak and D. Gerling, ""Review of Position Estimation Methods for IPMSM Drives Without a Position Sensor Part II: Adaptive Methods," in XIX International Conference on Electrical Machines - ICEM 2010, 2010.

[8] O. Benjak and D. Gerling, "Review of Position Estimation Methods for IPMSM Drives Without a Position Sensor Part I: Nonadaptive Methods," in XIX International Conference on Electrical Machines - ICEM 2010, 2010.

[9] A. Essalmi, H. Mahmoudi, A. Abbou, A. Bennassar and Y. Zahraoui, ""DTC of PMSM based on artificial neural networks with regulation speed using the fuzzy logic controller," REsearch Gate, p. 879–883, 2014.

[10] A. T. Umoette, O. I. Okoro and I. E. Davidson, "Performance analysis of a 10hp three phase induction motor using classical and finite-elements for varying load conditions," in In 2021 IEEE PES/IAS PowerAfrica, 2021.

[11] A. Sudhakar and M. V. Kumar, "Torque Ripple Reduction in Direct Torque Control Based Induction Motor using Intelligent Controllers," " Journal of The Institution of Engineers (India), vol. 96, no. 3, p. 297–304, 2014.

[12] F. Niu, B. Wang, A. Babel, K. Li and E. Strangas, ""Comparative Evaluation of Direct Torque Control Strategies for Permanent Magnet Synchronous Machines," IEEE Transactions on Power Electronics, vol. 31, no. 2, p. 1408–1424, 2016.

[13] P. Pillay and R. Krishnan, " Application characteristics of permanent magnet synchronous and brushless dc motors for servo drives," IEEE Transactions on Power Electronics, vol. 27, no. 5, 1991.

[14] S. Lin, T. X. Wu, L. Zhou, F. Moslehy, J. Kapat and L. Chow, "Modeling and Design of Super High Speed Permnanen Magnet Synchronous Motor (PMSM)," in 2008 IEEE National Aerospace and Electronics Conference , Dayton, OH, USA, 2008.

[15] V. Joshi, S. Jeevanand and H. Mohan, "Modeling and Analysis of MRAS based Speed Sensorless Control for PMSM Drive," in 2021 IEE 8th Uttar Pradesh Section International Conference on Electrical, Electronics and Computer Engineering (UPCON), Dehradun, India, 2021.

[16] S. Sakunthala, R. Kiranmayi and P. N. Mandadi, "Investigation of PI and Fuzzy Controllers for Speed Control of PMSM Motor Drive," in 2018 International Conference on Recent Trends in Electrical, Control and Communication (RTECC) , Malaysia,Malaysia, 2018.

[17] Q. Shen, Z. Zhou, S. Li, X. Liao, T. Wang, X. He and J. Zhang, "Design and analysis of the high-speed permanent magnet motors: A review on the state of the art," Machines, vol. 10, no. 7, p. 549, 2022.

[18] M. Torrent, J. I. Perat and J. A. Jiménez, " Permanent magnet synchronous motor with different rotor structures for traction motor in high speed trains," Energies, vol. 11, no. 6, p. 1549, 2018.

[19] U. S. Ekop, E. Okpo, A. T. Umoette, I. S. Etim and O. I. Jackson, "Application of Intelligent Overcurrent Relays for Real-time Protection of Induction Motor under Fault Conditions," Journal of Engineering Research and Reports, , vol. 27, no. 3, pp. 489-510, 2025.

[20] U. O. Innocent, I. E. Nkan, E. E. Okpo and O. I. Okoro, "Dynamic response evaluation of a separately excited dc motor," Nigeria Journal of Engineering, vol. 28, no. 2, pp. 56-61, 2021.

[21] I. Petrov, D. Egorov, J. Link, R. Stern, S. Ruoho and J. Pyrhönen, "Hysteresis losses in different types of permanent magnets used in PMSMs," IEEE Transactions on Industrial electronics, vol. 64, no. 3, pp. 2502-2510, 2016.

[22] A. T. Umoette, O. I. Okoro and I. E. Davidson, "Speed Performance Enhancement and Analysis of a Three Phase Induction Motor Driving a Pump Load using Vector Control Technique," in In 2022 IEEE PES/IAS PowerAfrica, 2022.

[23] W. S. Jung, H. K. Lee, Y. K. Lee, S. M. Kim, J. I. Lee and J. Y. Choi, "Analysis and comparison of permanent magnet synchronous motors according to rotor type under the same design specifications," Energies, vol. 16, no. 3, p. 1306, 2023.

[24] M. Gedıkpinar, "Design and implementation of a self-starting permanent magnet hysteresis synchronous motor for pump applications," IEEE Access, vol. 7, pp. 186211-186216, 2019.

[25] U. I. Ukut, A. T. Umoette and N. Okpura, "Fast Decoupled Load Flow Analysis Of IEEE 33 Bus Distribution System," Journal of Multidisciplinary Engineering Science Studies (JMESS) ISSN, vol. 9, no. 1, 2023.

[26] C. Ma, S. Zhou, N. Yang, M. Degano, C. Gerada, J. Fang and Q. Liu, "Characteristic analysis and direct measurement for air gap magnetic field of external rotor permanent magnet synchronous motors in electric vehicles," IET Electric Power Applications, vol. 14, no. 10, pp. 1784-1794, 2020.

[27] E. E. Okpo, I. E. Nkan, J. Odion and A. L. Jack, "Induction Motor Voltage Variation and Fault Adaptation in Submarines," Journal of Engineering Research and Reports, vol. 26, no. 12, pp. 286-304, 2024.

[28] A. T. Umoette, U. J. Paul and E. A. Ubom, "Energy audit and standalone solar power generation design for Akwa Ibom State University Main Campus. Energy," Journal of Science and Technology (IMJST) , vol. 8, no. 6, 2023.

[29] H. C. Idoko, U. B. Akuru, R. J. Wang and O. Popoola, "Potentials of brushless stator-mounted machines in electric vehicle drives—a literature review," World Electric Vehicle Journal, vol. 13, no. 5, p. 93, 2022.

[30] C. O. Omeje and C. U. Eya, " A comparative braking scheme in auto-electric drive systems with permanent magnet synchronous machine," International Journal of Applied, vol. 11, no. 4, pp. 251-263, 2022.

[31] C. S. Ezeonye, I. K. Onwuka, O. Oputa and P. I. Obi, "A Study of Motor Sensitivity to Parameters Variation in Exterior Permanent Magnet Synchronous Motor," Bayero Journal of Engineering and Technology, vol. 18, no. 2, pp. 84-94, 2023.

[32] C. O. Omeje, A. O. Salau and C. U. Eya, "Dynamics analysis of permanent magnet synchronous motor speed control with enhanced state feedback controller using a linear quadratic regulator," Heliyon, vol. 4, p. 10, 2024.

[33] J. O. Owuor, J. L. Munda and A. A. Jimoh, "An Optimally Controlled Variable Output Wound Rotor Synchronous Machine," Int. J. Electr. Energy, vol. 4, pp. 54-61, 2016.

[34] F. E. Effiong, A. T. Umoette and K. J. Oyadinrin, "3. Development Of Fussy Logic Approach For Fault Current Diagnosis And Classification In Power Lines," Journal of Multidisciplinary Engineering Science Studies (JMESS), vol. 8, no. 1, 2 , 022.

[35] A. Shahat and H. Shewy, " Permanent magnet synchronous motor dynamic modeling with genetic algorithm performance improvement," International Journal of Engineering, Science and Technology, vol. 2, no. 2, pp. 93-106, 2010.

[36] P. Krause, O. Wasynczuk, S. Sudhoff and S. Pekarek, Analysis of Electric Machinery and Drive Systems, 3. edition, Ed., New : John Wiley & Sons, Inc, 2013.

[37] F. A. Patakor, M. Sulaiman and Z. Ibrahim, "Performance of sliding mode control for three phase induction motor," in In 2010 International Conference on Science and Social Research (CSSR 2010), 2010.

[38] H. Mohan, M. K. Pathak and S. K. Dwivedi, "Reactive power based speed control of induction motor drive using fuzzy logic for industrial applications," in In 2020 IEEE International Conference on Power Electronics, Smart Grid and Renewable Energy (PESGRE2020), IEEE, 2020.

[39] Z. Yang, C. Lu, X. Sun, J. Ji and Q. Ding, "Study on active disturbance rejection control of a bearingless induction motor based on an improved particle swarm optimization–genetic algorithm.," IEEE Transactions on Transportation Electrification, vol. 7, no. 2, pp. 694-705, 2020.